

STABILITY ANALYSIS FOR URBAN TRAFFIC EVOLUTION PROCESS USING TEMPORAL TRAFFIC STATE PATTERNS

Longjian WANG¹, Yonggang WANG^{2*#}, Longfei WANG³

^{1,2}College of Transportation Engineering, Chang'an University, Xi'an, China

³School of Engineering, Dali University, Dali, China

Submitted 5 August 2020; resubmitted 27 February 2021, 31 August 2021; accepted 5 October 2021

Abstract. Recognizing the stability of the traffic evolution process of urban traffic networks has been an important consideration in traffic evolution research. However, little work has been conducted on identifying and associating temporal Traffic State Pattern (TSP) with the traffic evolution process. By clustering multi-dimensional traffic time series, we attempted to map the traffic evolution process into massive transitions of consecutive TSPs. Through the statistics of the time distribution of the transitions, we then defined the stability coefficient to conduct a quantitative analysis of the traffic evolution process. An empirical study using 30 days of traffic flow rate data of multiple road sections from the network of Nanshan District (Shenzhen, China) was carried out. Numerical results indicated that the traffic evolution process experienced obvious nonlinear changes at different periods of the day, but presented a regular cycle characteristic from morning till night. Further, with consideration of different travel purposes and traffic features on weekday and weekend, more traffic dynamics was extracted, which would be conducive to understand the complex behaviour of traffic evolution process.

Keywords: traffic flow, stability analysis, evolution process, traffic state, urban traffic.

Notations

- ATST – abnormal traffic state transition;
- ATSPT – abnormal TSP transition;
- HATSPT – heavy abnormal TSP transition;
- LWR – Lighthill, Whitham and Richards traffic flow model;
- MATSPT – medium abnormal TSP transition;
- MFD – macroscopic fundamental diagram;
- NTSPT – normal TSP transition;
- NTST – normal traffic state transition;
- SOM – self-organizing maps;
- TSP – traffic state pattern;
- TSPG – TSP group;
- TSPT – TSP transition;
- TSPTR – TSP transition relation;
- TSPTRN – TSP transition relation network.

Introduction

Nowadays, the increasing contradiction between supply and demand in urban transportation makes traffic congestion one of the serious problems that most cities need to face (Beaudoin *et al.* 2018). Traffic congestion contains 2 types: (1) occasional and (2) recurrent. Occasional congestion is irregular and may occur at any time and any place, which is caused by unexpected conditions such as traffic events. Recurrent congestion has temporal periodicity and high spatial similarity, which is caused by insufficient infrastructure supply (An *et al.* 2016). Previous studies have confirmed that traffic congestion is the result of instability and phase transition in the traffic flow dynamics (Ghadami *et al.* 2022). To analyse the characteristics of traffic congestion, the traffic flow is abstracted into TSP (Lan *et al.* 2008). The investigation of TSP can help analyse the causes of congestion and suggest delicacy management measures to ensure traffic safety and smoothness. Therefore, TSP has become an interesting topic that has attracted many researchers.

*Corresponding author. E-mail: wangyg@chd.edu.cn

#Editor of the TRANSPORT – the manuscript was handled by one of the Associate Editors, who made all decisions related to the manuscript (including the choice of referees and the ultimate decision on the revision and publishing).

Depending on the purpose of the study and the data available, researchers use different metrics to characterize TSPs, including traffic flow (Shen, Zhang 2009; Zhang *et al.* 2016), density (Treiber, Kesting 2012), and velocity (Banaei-Kashani *et al.* 2011), etc. As detection technologies evolve and the scale of traffic data explodes, the scope of research is gradually expanding from intersections (Li *et al.* 2019) and corridors (Lan *et al.* 2008) to small areas (Zhu *et al.* 2016) and entire cities (Anbaroglu *et al.* 2014; Yang *et al.* 2018). Accompanying this expansion is the evolution of algorithms. The LWR model described the equilibrium speed-concentration relationship, which has been widely applied in the estimation of traffic state (Lighthill, Whitham 1955; Richards 1956). The acceleration is introduced into the LWR model to obtain a higher-order continuum model, the Payne (1971) model. Then many improved models (Daganzo 1995; Zhang 1998) emerged to facilitate the development of higher-order continuum models. With the interest in the traffic state of the global road network, Daganzo and Geroliminis (2008) defined the MFD. The MFD model is obtained by statistically analysing the historical data of the road network to get the relationship between different parameters such as density, velocity, and flow, etc. With the increase of data volume and the high demand for data processing ability, machine learning models have gained popularity among scholars. Clustering is one of the machine learning models that have been widely utilized in analysing traffic states, revealing hidden patterns in huge traffic data, and realizing traffic state classification. The SOM (Kohonen 1982) is one of the representative clustering algorithms. SOM uses unsupervised learning to map higher dimensional inputs onto the lower dimensional grid while preserving the topological ordering present in the input space (García-Rois, Burguillo 2017). Chen *et al.* (2008) used SOM to cluster traffic flow vectors to analyse the characteristics of multi-dimensional traffic flow time series and predict future trends. Then ample researches (Andrienko *et al.* 2010; Chiou *et al.* 2014; Gu *et al.* 2020) verified that the SOM can effectively discriminate congestion using real traffic data.

Meanwhile, previous studies analysed the spatial-temporal characteristics of TSPs. Kim and Keller (2008) investigated the dynamic flow density relationship based on traffic state classification. Zhang *et al.* (2016) analysed the geographic distribution of TSPs, pattern shifts at different times-of-day, and pattern fluctuations over different days. Zhu *et al.* (2016) used the hidden Markov model to represent the dynamic transition process of traffic state and analysed the law of dynamic transition in traffic state of the urban road network under the influence of traffic information. Yang *et al.* (2018) analysed the spatial correlation of urban traffic states to identify evolutionary patterns. Although some researchers have analysed the spatio-temporal evolutionary relationships of TSPs, the stability during the evolutionary process has been ne-

glected, and there are still research gaps to explore further.

Inspired by this, the main purpose of this research is to construct an analysis model of TSP stability from the perspective of macroscopic traffic flow and to investigate the distinct regularity of the traffic state evolution process. The traffic evolution process is regarded as massive transitions of successive TSPs. The stability analysis of the traffic evolution process then becomes the transition analysis of TSPs. In our previous paper (Wang *et al.* 2014), we defined TSP through clustering multidimensional traffic time series using SOM and construct a pattern transition network model. Then we analysed the temporal characteristics and distinct regularity in the traffic evolution process, including preference, activity, and attractiveness.

In this paper, we further study the temporal characteristics of the traffic evolution process, focusing on stability modelling and analysis. We construct a simple analysis model of TSP stability to quantitatively analyse the stability of the traffic evolution process. We attempt to gain insight into the stability of the traffic evolution process in urban traffic networks. By investigating the stability of traffic dynamics in the temporal domain, we can understand the distinctive features of traffic flow evolution and fluctuation, and further develop effective traffic management measures and ITS applications. Furthermore, we believe that this analysis provides a new way to measure and quantify the traffic evolution process and improves the understanding of the complex behaviour of the temporal evolution features of traffic patterns. Ultimately, flow rate data of multiple road sections from the network of Nanshan District (Shenzhen, China), were used to illustrate the effectiveness of the proposed method.

The remaining parts are organized as follows. Section 1 introduces the analysis model of TSP stability. Then the empirical data and road network are shown in Section 2. In Section 3, the analytical results are discussed. Finally, the conclusions of our work are presented in the final section.

1. Analysis model of TSP stability

To describe the transition process of traffic state, a basic network model for traffic evolution analysis of urban regional networks is proposed. The transition process and evolutionary characteristics of traffic state are analysed from a quantitative perspective.

One traffic parameter (such as traffic volume, speed, occupancy, delay, V/C , etc.) can be selected to describe the traffic state of the road section. We select traffic flow rate as the input parameter. The n -dimensional vector $F(t) = [f_1(t), f_2(t), \dots, f_n(t)]^T$ was used to represent traffic state within the time interval t , where $f_i(t)$ is the flow rate of the i th road section within the time interval t and n is the total number of road sections. Then multiple traffic state classifications can be obtained by clustering traffic states, each of which is composed of a set of

traffic states, that is, TSP, denoted by P . Here Kohonen's SOM (Kohonen 1982; Chen et al. 2008; Chiou et al. 2014) algorithm was used to cluster TSPs. For a more detailed theoretical model of SOM, see Chen et al. (2008). The results of the above study have proven the effectiveness of this method, and our previous study (Wang et al. 2014) has also proved it is effective and reasonable. Then the mean fitting method was used to fitting traffic states, and the characteristic state $F_C^P(t) = [f_1^P(t), f_2^P(t), \dots, f_n^P(t)]^T$ can be obtained, where $f_i^P(t)$ is the mean value of flow rate of the i th road section of all traffic states within P .

Our previous study (Wang et al. 2014) defined several network models, such as TSPTR $R_{A \rightarrow B} = P_A \rightarrow P_B$ and TSPTRN $G = (P, R)$, where R is all transition relation sets. Based on this, we give the following definition.

Definition 1. If P_A and P_B are TSPs, $F(t_1) \in P_A$, $F(t_2) \in P_B$, t_1 and t_2 are adjacent periods, then there exists a TSPT between $F(t_1)$ and $F(t_2)$, denoted as $T_{A \rightarrow B}$.

Definition 2. The variation coefficient α_i^c of traffic state in adjacent periods of road section i can be expressed as:

$$\alpha_i^c = \left| \frac{\Delta_i^c}{\max(f_i(t)) - \min(f_i(t))} \right|, \quad (1)$$

where: Δ_i^c is the variation of traffic flow rate in adjacent periods of road section i ; $\max(f_i(t))$, $\min(f_i(t))$ respectively represent the maximum flow rate and minimum flow rate of the i th road section within the time interval t in a day. Define α_i is the anomaly detection threshold value for ATST. If $\alpha_i^c < \alpha_i$, then there exists a NTST for the i th road section. If $\alpha_i^c \geq \alpha_i$, then exists an ATST for the i th road section.

Definition 3. For $T_{A \rightarrow B}$, $R_{A \rightarrow B} = P_A \rightarrow P_B$, the total number of ATSTs of all road sections in $T_{A \rightarrow B}$ is denoted as $\Psi(T_{A \rightarrow B})$. If $0 \leq \Psi(T_{A \rightarrow B}) \leq \beta_M$, then $T_{A \rightarrow B}$ is NT-SPT. If $\beta_M < \Psi(T_{A \rightarrow B}) < \beta_H$, then $T_{A \rightarrow B}$ is MATSPT. If $\Psi(T_{A \rightarrow B}) \geq \beta_H$, then $T_{A \rightarrow B}$ is HATSPT. Where, β_M and β_H are respectively the threshold value of medium and heavy ATST of $R_{A \rightarrow B}$.

The traffic evolution process is composed of massive consecutive traffic state transitions. The more is MATSPT and HATSPT, the less is NT-SPT, and the weaker the stability. Therefore, the statistics results to the count and time distribution of NT-SPT, MATSPT, and HATSPT of the traffic state transitions can visually reflect the stability of the dynamic traffic evolution process. Therefore, we will define the stability coefficient, which shows different levels of exponential decreases as the count of MATSPT and HATSPT increases. We believe the more the count of ATST (the sum of MATSPT and HATSPT), the faster the stability decrease.

Definition 4. Given a specified time duration t , the stability coefficient C_t^S in the traffic evolution process can be expressed as:

$$C_t^S = \omega_M \cdot e^{-Ave_h(N_t^M)} + \omega_H \cdot e^{-Ave_h(N_t^H)}, \quad (2)$$

where: N_t^M and N_t^H are respectively the total count of all MATSPTs and HATSPTs within a given specified time duration t ; ω_M and ω_H are the weight of effects of MATSPT and HATSPT respectively; the function $Ave_h(\cdot)$ is used to compute the average count of MATSPT and HATSPT per hour of the day. The average count of MATSPT is taken as an example to calculate as the following:

$$Ave_h(N_t^M) = \frac{60 \cdot N_t^M}{t}, \quad (3)$$

where: time duration is t [days]; the average lasting time of MATSPT is t_M [min].

From Equation (2), it can be seen that C_t^S decreases as the count of MATSPT and HATSPT increases. Therefore, the larger C_t^S , the stronger the stability.

2. Experimental data

In this paper, the regional road network in Nanshan District is selected as the experimental road network. The road network topology is shown in Figure 1. Taking intersections as nodes, the regional road network is divided into 35 road sections, numbered 1...35 respectively. The real flow rate datasets of the road section in Nanshan District are analysed. The flow rates datasets were obtained from our previous study (Wang et al. 2014), a total of 30 days of flow data. The period of this experimental study is from 6:00 to 24:00, with the unit time interval is 5 min. Each road section has $12 \times 18 \times 30 = 6480$ data samples. Then a 35-dimensional series with a length of 6480 was constructed.

We selected 2 days of data for training and found that the SOM with 8×8 neurons worked best. Because SOM with fewer neurons would blur the input spatial relationships, resulting in discrete relationships among the TSPs. While SOM with more neurons would increase the complexity and computation time, and also make it difficult

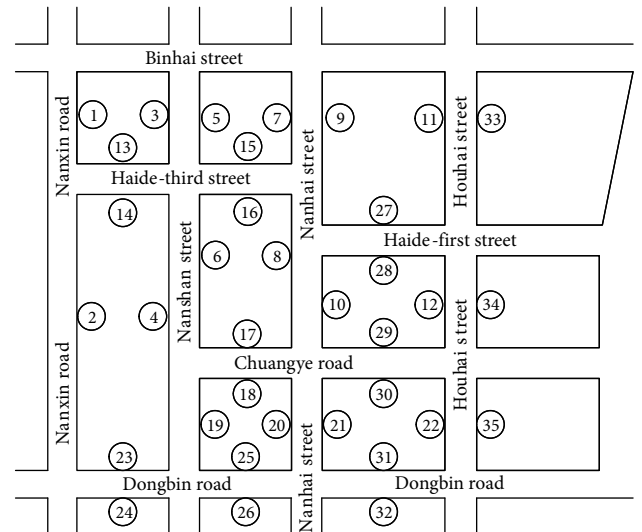


Figure 1. Road network topology of Nanshan District

for visualization and analysis. Therefore, a well-trained 8×8 SOM network was used to cluster flow rate data, and 64 clusters were obtained. There are 4 TSPG, represented by “A”, “B”, “C”, and “D” respectively. Ranked according to the degree of congestion is A > B > C > D. For a more detailed clustering result of TSP, see our previous study (Wang *et al.* 2014). Each cluster represents a TSP with 35-dimensions.

3. Experimental analysis

3.1. Generation of TSPTRN

Considering the different travel purposes, traffic demand, and traffic distribution characteristics, we conduct our experimental analysis on weekdays and weekends respectively. The TSPTRN and detailed time distribution after mapping of each TSP of weekdays are respectively shown in Figures 2 and 3. The TSPTRN and detailed time distribution after mapping of each TSP of weekends are respectively shown in Figures 4 and 5.

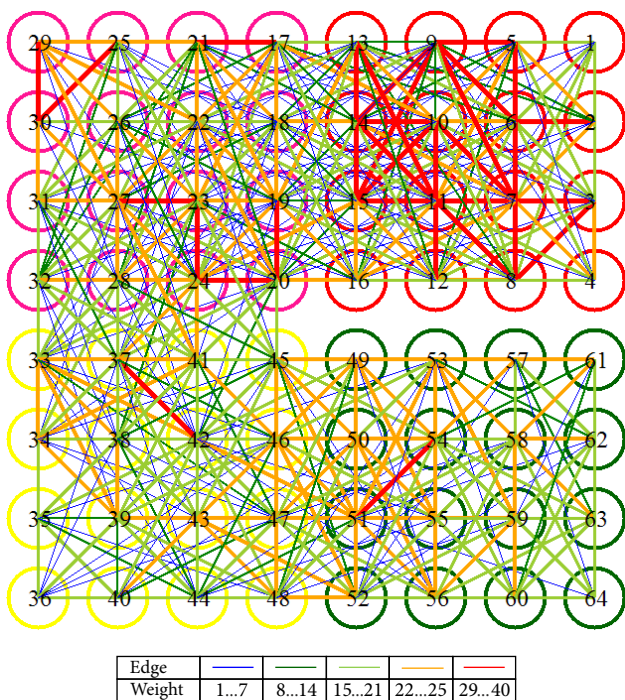


Figure 2. TSPTRN of Nanshan District on weekdays (22 days)

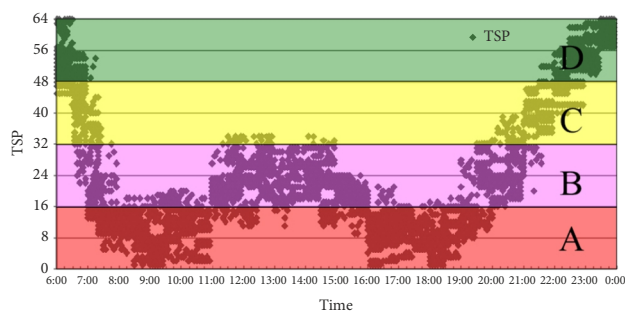


Figure 3. Time distribution of TSP on weekdays (22 days)

We can see that the evolution process among the TSPGs during a whole day follows a common sequence that is <D → C → B → A → B → A → B → C → D> on both weekdays and weekends, as shown in Table 1. This sequence of time distribution just indicates that macroscopic traffic operation of the road network has a strong regularity and the traffic operation is stable within a certain period.

3.2. Analysis of stability

We set $\beta_M = 5$ and $\beta_H = 9$ based on the median and 90% quantile of the total count of ATST. In addition, we believe that it is very abnormal if the traffic flow rate changes largely in a short period, so we set $\alpha_i = 0.4$. Then the counts of NTSPT, MATSPT, and HATSPT can be obtained and the time distributions on weekdays and weekends are respectively shown in Figures 6 and 7. To cover the whole traffic evolution process and make a comprehensive analysis of stability, we conduct 2 steps of analysis respectively within and between TSPGs according to Table 1.

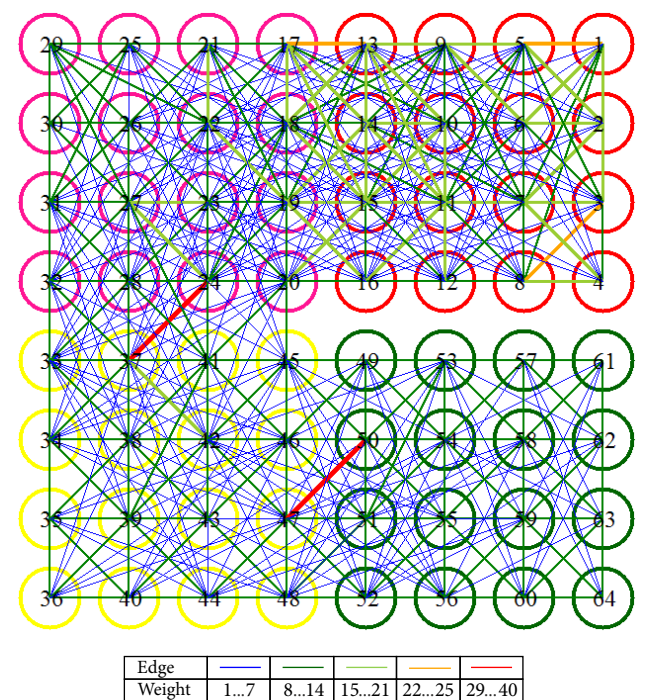


Figure 4. TSPTRN of Nanshan District on weekends (8 days)

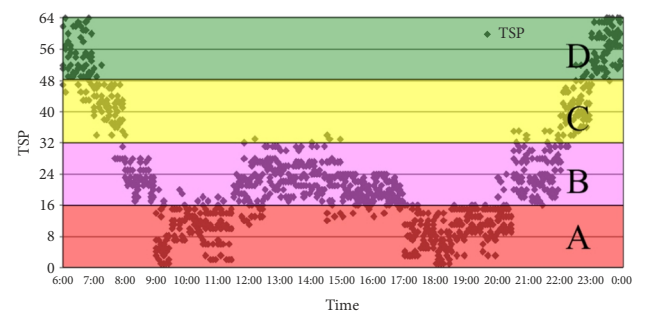


Figure 5. Time distribution of TSP on weekends (8 days)

Table 1. Evolution sequence and time distribution of the TSPGs

TSPG	Average start time		Average end time		Average lasting time		Time proportion	
	weekday	weekend	weekday	weekend	weekday	weekend	weekday	weekend
D	06:00	06:00	06:25	07:05	25 min	1 h 5 min	2.31%	6.02%
C	06:25	07:05	06:55	08:10	30 min	1 h 5 min	2.78%	6.02%
B	06:55	08:10	07:30	09:05	35 min	55 min	3.24%	5.09%
A	07:30	09:05	11:05	11:35	3 h 35 min	2 h 30 min	19.91%	13.89%
B	11:05	11:35	16:10	17:10	5 h 5 min	5 h 35 min	28.24%	31.02%
A	16:10	17:10	19:35	20:35	3 h 25 min	3 h 25 min	18.98%	18.98%
B	19:35	20:35	21:10	22:05	1 h 35 min	1 h 30 min	8.80%	8.33%
C	21:10	22:05	22:05	23:10	55 min	1 h 5 min	5.09%	6.02%
D	22:05	23:10	0:00	0:00	1 h 55 min	50 min	10.65%	4.63%

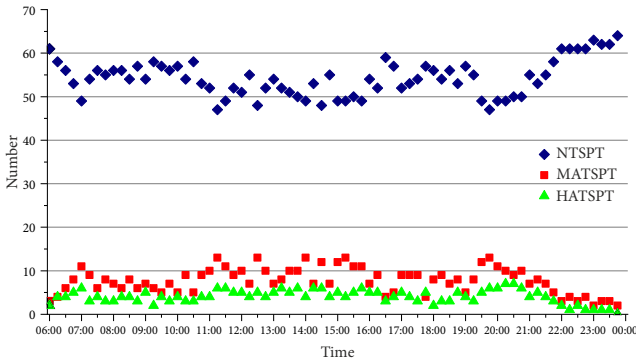


Figure 6. Time distribution of NTSPT, MATSPT, and HATSPT on weekdays (22 days)

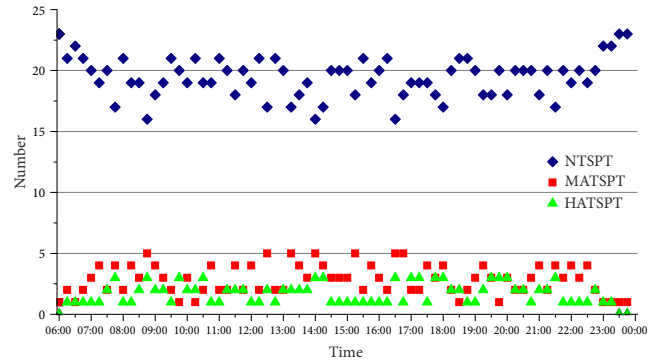


Figure 7. Time distribution of NTSPT, MATSPT, and HATSPT on weekends (8 days)

3.2.1. Stability of TSPT within TSPG

The average count of MATSPT and HATSPT per hour of the day within TSPG is shown in Table 2. The average count of MATSPT in TSPG “D” that 1st appeared on weekdays is taken as an example to calculate using Equation (3), and the calculation process is as follows:

$$Ave_h(N_t^M) = \frac{6 \cdot 60}{22 \cdot 25} = 0.65.$$

After merging the same TSPG, we get the combined-average value of $Ave_h(N_t^M)$ and $Ave_h(N_t^H)$, and thus the C_t^S can be obtained, as shown in Table 3. The calculation process of the combined-average value of $Ave_h(N_t^M)$ in TSPG “A” on weekdays is given as an example:

$$Ave_h(N_t^M) = \frac{1.23+1.34}{2} = 1.285. \text{ The calculation process}$$

of C_t^S the in TSPG “A” on weekdays is given as an example: $C_t^S = 0.65 \cdot e^{-1.285} + 0.95 \cdot e^{-0.66} = 0.6708$.

From Table 3, we can see that no matter of weekday or weekend, the stability results of each TSPG calculated by the stability coefficient C_t^S formula is: $D > A > C > B$. The C_t^S value of TSPG “D” was much higher than the other TSPGs. This is mainly because the TSPs in “D” happened in the early morning and late at night. In these periods, the traffic is basically at the state of free travel, and the traffic operation state is quite smooth and stable in the whole day. It is also corroborated by Figures 6 and 7, as the number of MATSPT and HATSPT was the lowest during this period of the day.

Besides, TSPG “A” had also shown relatively higher stability than “B” and “C”. This is due to the TSPs in TSPG “A” are in the morning and evening peak hours, which are congested periods with relatively stable traffic demand and traffic distribution without significant disturbance. Moreover, the traffic state of each road is in the “saturated” or “nearly saturated” condition, and the change interval of the traffic state is limited.

The stability of TSPG “B” is the smallest. Because for each pattern of “B”, the traffic states of each road were all in “nearly saturated” condition, and thus have larger variations spaces and change possibilities than that of “A”, “C” and “D”. Moreover, the traffic state transition of the whole network is in a period of extreme activity and fluctuation, with relatively unstable traffic demand and irregular traffic distribution. It can also be demonstrated by Figures 6 and 7, as the number of MATSPT and HATSPT is the highest during this period of the day.

3.2.2. Stability of TSPT between TSPGs

According to Table 1, the evolution in a whole day experienced 9 TSPGs, so there are 8 Transition periods between TSPGs, which are $\langle D \rightarrow C \rangle$, $\langle C \rightarrow B \rangle$, $\langle B \rightarrow A \rangle$, $\langle A \rightarrow B \rangle$, $\langle B \rightarrow A \rangle$, $\langle A \rightarrow B \rangle$, $\langle B \rightarrow C \rangle$ and $\langle C \rightarrow D \rangle$. Each Transition period is formed by the last 15mins of the start TSPG and the early 15 min of the end TSPG. We set each Transition period to 30 min, which is formed by the last 15 min of the start TSPG and the early

15 min of the end TSPG. The stability coefficient C_t^S is obtained as shown in Table 4. The calculation process of $Ave_h(N_t^M)$ in $\langle D \rightarrow C \rangle$ on weekdays is given as an example: $Ave_h(N_t^M) = \frac{10 \cdot 60}{22 \cdot 30} = 0.91$. The calculation process of C_t^S the in $\langle D \rightarrow C \rangle$ on weekdays is given as an example: $C_t^S = 0.65 \cdot e^{-0.91} + 0.95 \cdot e^{-0.64} = 0.7626$. The remaining values can be calculated in the same way as above.

$\langle B \rightarrow A \rangle$ and $\langle A \rightarrow B \rangle$ are respectively the formation period and dissipating period of morning and evening peak hours. In these periods, the traffic states of each road were less in “saturated” condition (i.e., the percentage of travel speed to basic free-flow speed is less than or equal to 0.3, $\frac{v}{v_f} \leq 0.3$ (TRB 2010)) and more in “nearly saturated” condition (i.e., $0.3 < \frac{v}{v_f} \leq 0.4$ (TRB 2010)). When abnormal events such as traffic congestion or accidents

occur, the adverse effects can spread rapidly. Therefore, the stability of the transitions between TSPG “A” and “B” is smaller than that of transitions among “B”, “C”, and “D”. Although the transitions occur between TSPG “A” and “B”, the stability of most transitions is closer to “B” than “A”. Because the value of stability coefficient in stages 4, 5, and 6 is closer to the stability coefficient of “B”. Let’s take stage 4 on weekdays as an example: the absolute value between the stability coefficient in stage 4 and TSPG “A” is $|0.5163 - 0.6708| = 0.1545$, the absolute value between the stability coefficient in stage 4 and TSPG “B” is $|0.5163 - 0.4701| = 0.0462$, and $0.1545 > 0.0462$, so the stability in stage 4 is closer to “B” than “A”. This shows that the transition stability between “A” and “B” is low.

Compared with $\langle B \rightarrow A \rangle$ and $\langle A \rightarrow B \rangle$, the stability of $\langle B \rightarrow C \rangle$ and $\langle C \rightarrow B \rangle$ is a litter larger. Although the stability of TSPG “C” and “B” is relatively small, as “B” is in “nearly saturated” condition and “C” is in “unsatu-

Table 2. The average count of MATSPT and HATSPT per hour of the day within TSPG

TSPG	Weekday (22 days)				Weekend (8 days)			
	N_t^M	$Ave_h(N_t^M)$	N_t^H	$Ave_h(N_t^H)$	N_t^M	$Ave_h(N_t^M)$	N_t^H	$Ave_h(N_t^H)$
D	6	0.65	5	0.55	7	0.81	3	0.35
C	12	1.09	8	0.73	13	1.50	8	0.92
B	23	1.79	11	0.86	14	1.91	7	0.95
A	97	1.23	50	0.63	24	1.20	18	0.90
B	205	1.83	104	0.93	77	1.72	37	0.83
A	101	1.34	52	0.69	36	1.32	30	1.10
B	63	1.81	38	1.09	18	1.50	11	0.92
C	26	1.29	14	0.69	13	1.50	5	0.58
D	23	0.55	8	0.19	3	0.45	2	0.30

Table 3. The stability coefficient within TSPG

TSPG	Weekday (22 days), $\omega_M = 0.65, \omega_H = 0.95$			Weekend (8 days), $\omega_M = 0.65, \omega_H = 0.95$		
	$Ave_h(N_t^M)$	$Ave_h(N_t^H)$	C_t^S	$Ave_h(N_t^M)$	$Ave_h(N_t^H)$	C_t^S
A	1.285	0.66	0.6708	1.25	0.87	0.5842
B	1.81	0.96	0.4701	1.67	0.94	0.4935
C	1.19	0.71	0.6648	1.63	0.76	0.5716
D	0.60	0.37	1.0129	0.63	0.32	1.0360

Table 4. The Stability coefficient between TSPGs

Stage	TSPG transition	Weekday (22 days), $\omega_M = 0.65, \omega_H = 0.95$					Weekend (8 days), $\omega_M = 0.65, \omega_H = 0.95$				
		N_t^M	$Ave_h(N_t^M)$		$Ave_h(N_t^H)$	C_t^S	N_t^M	$Ave_h(N_t^M)$	N_t^H	$Ave_h(N_t^H)$	C_t^S
1	$\langle D \rightarrow C \rangle$	10	0.91	7	0.64	0.7626	3	0.75	2	0.50	0.8832
2	$\langle C \rightarrow B \rangle$	16	1.45	9	0.82	0.5709	6	1.50	3	0.75	0.5938
3	$\langle B \rightarrow A \rangle$	17	1.55	10	0.91	0.5204	7	1.75	3	0.75	0.5617
4	$\langle A \rightarrow B \rangle$	15	1.36	11	1.00	0.5163	5	1.25	4	1.00	0.5357
5	$\langle B \rightarrow A \rangle$	19	1.73	11	1.00	0.4647	6	1.50	5	1.25	0.4172
6	$\langle A \rightarrow B \rangle$	16	1.45	10	0.91	0.5349	6	1.50	4	1.00	0.4945
7	$\langle B \rightarrow C \rangle$	14	1.27	9	0.82	0.6010	5	1.25	3	0.75	0.6350
8	$\langle C \rightarrow D \rangle$	11	1.00	8	0.73	0.6969	4	1.00	3	0.75	0.6879

rated" condition, the traffic states of each road can still pursue smooth and stable transition in the consecutive time interval during the transition between "B" and "C". What's more, even abnormal event cannot lead to large-scale spread adverse effects. Although the transitions occur between "B" and "C", the stability is closer to "C" than "B". That is, the transition stability between "B" and "C" is relatively higher.

The stability of $\langle D \rightarrow C \rangle$ and $\langle C \rightarrow D \rangle$ is the largest of all the transitions between TSPGs. This is because the traffic states of each road were almost at the state of free travel or "unsaturated" condition with the traffic operation quite natural and stable during the transitions with no obvious significant changes even in case of abnormal traffic events.

Conclusions

Accurate and in-depth analysis of the stability of the traffic state evolution process is a necessary condition to alleviate traffic congestion in urban. Therefore, we proposed a novel model to analyse the stability of the traffic state evolution process in urban regional road networks from a macroscopic perspective. We mapped the traffic evolution process into transitions of consecutive TSPs and defined stability coefficient, which can be used to conduct a quantitative analysis of the traffic evolution process through the statistics to the time distribution of the transitions.

To illustrate the applicability and effectiveness of the proposed model, the road network of Nanshan District (Shenzhen, China) is taken as an example to analyse and verify.

The experimental results show that the traffic evolution process experienced obvious nonlinear changes at different periods of the day, but presented a regular cycle characteristic from morning till night. Whether it is a weekday or a weekend, the stability is TSPG "D", "A", "C", and "B" in descending order. Besides, the stability of the transitions between TSPG "A" and "B" is the smallest, followed by the stability of the transitions between "B" and "C", and the transitions between "C" and "D" is the most stable.

According to our empirical results, the proposed analytical method permits mining the change regulation and influence factors of stability on different periods of the day and extracting more information about traffic dynamics with the consideration of different travel purposes and traffic features on weekdays and weekends. We believe that this paper may provide a valuable reference for refined traffic control in urban areas, as well as traffic safety and move smoothly under the background of big data and automated vehicles.

However, it should be noted that compared with the stability analysis in the temporal domain, spatiotemporal stability analysis will be more valuable. Therefore, one challenge for our further study is to develop spatiotemporal stability analysis methods and discuss the threshold setting in detail.

Acknowledgements

This work was supported by the Natural Science Foundation of Shaanxi Province, China (Grant No 2020JM-252).

Author contributions

Longjian Wang conceived the study and wrote the 1st draft of the paper.

Yonggang Wang was responsible for the design of the data analysis.

Longfei Wang was responsible for data collection.

All authors reviewed, edited and approved the paper.

Disclosure statement

This paper do not have any competing financial, professional, or personal interests from other parties.

References

- An, S.; Yang, H.; Wang, J.; Cui, N.; Cui, J. 2016. Mining urban recurrent congestion evolution patterns from GPS-equipped vehicle mobility data, *Information Sciences* 373: 515–526. <https://doi.org/10.1016/j.ins.2016.06.033>
- Anbaroglu, B.; Heydecker, B.; Cheng, T. 2014. Spatio-temporal clustering for non-recurrent traffic congestion detection on urban road networks, *Transportation Research Part C: Emerging Technologies* 48: 47–65. <https://doi.org/https://doi.org/10.1016/j.trc.2014.08.002>
- Andrienko, G.; Andrienko, N.; Bremm, S.; Schreck, T.; Von Landesberger, T.; Bak, P.; Keim, D. 2010. Space-in-time and time-in-space self-organizing maps for exploring spatiotemporal patterns, *Computer Graphics Forum* 29(3): 913–922. <https://doi.org/10.1111/j.1467-8659.2009.01664.x>
- Banaei-Kashani, F.; Shahabi, C.; Pan, B. 2011. Discovering patterns in traffic sensor data, in *IWGS'11: Proceedings of the 2nd ACM SIGSPATIAL International Workshop on GeoStreaming*, 1 November 2011, Chicago, IL US, 10–16. <https://doi.org/10.1145/2064959.2064963>
- Beaudoin, J.; Lin Lawell, C.-Y. C. 2018. The effects of public transit supply on the demand for automobile travel, *Journal of Environmental Economics and Management* 88: 447–467. <https://doi.org/10.1016/j.jeem.2018.01.007>
- Chen, Y.; Zhang, Y.; Hu, J. 2008. Multi-dimensional traffic flow time series analysis with self-organizing maps, *Tsinghua Science and Technology* 13(2): 220–228. [https://doi.org/10.1016/s1007-0214\(08\)70036-1](https://doi.org/10.1016/s1007-0214(08)70036-1)
- Chiou, Y.-C.; Lan, L. W.; Tseng, C.-M. 2014. A novel method to predict traffic features based on rolling self-structured traffic patterns, *Journal of Intelligent Transportation Systems: Technology, Planning, and Operations* 18(4): 352–366. <https://doi.org/10.1080/15472450.2013.806764>
- Daganzo, C. F. 1995. Requiem for second-order fluid approximations of traffic flow, *Transportation Research Part B: Methodological* 29(4): 277–286. [https://doi.org/10.1016/0191-2615\(95\)00007-z](https://doi.org/10.1016/0191-2615(95)00007-z)
- Daganzo, C. F.; Geroliminis, N. 2008. An analytical approximation for the macroscopic fundamental diagram of urban traffic, *Transportation Research Part B: Methodological* 42(9): 771–781. <https://doi.org/10.1016/j.trb.2008.06.008>

- García-Rois, J.; Burguillo, J. C. 2017. Topology-based analysis of self-organizing maps for time series prediction, *Soft Computing* 21(6): 1601–1618. <https://doi.org/10.1007/s00500-015-1872-5>
- Ghadami, A.; Doering, C.; Drake, J. M.; Rohani, P.; Epureanu, B. 2022. Stability and resilience of transportation systems: is a traffic jam about to occur?, *IEEE Transactions on Intelligent Transportation Systems* 23(8): 10803–10814. <https://doi.org/10.1109/TITS.2021.3095897>
- Gu, Y.; Wang, Y.; Dong, S. 2020. Public traffic congestion estimation using an artificial neural network, *ISPRS International Journal of Geo-Information* 9(3): 152. <https://doi.org/10.3390/ijgi9030152>
- Kim, Y.; Keller, H. 2008. Analysis of characteristics of the dynamic flow-density relation and its application to traffic flow models, *Transportation Planning and Technology* 31(4): 369–397. <https://doi.org/10.1080/03081060802334995>
- Kohonen, T. 1982. Self-organized formation of topologically correct feature maps, *Biological Cybernetics* 43(1): 59–69. <https://doi.org/10.1007/bf00337288>
- Lan, L. W.; Sheu, J.-B.; Huang, Y.-S. 2008. Investigation of temporal freeway traffic patterns in reconstructed state spaces, *Transportation Research Part C: Emerging Technologies* 16(1): 116–136. <https://doi.org/10.1016/j.trc.2007.06.006>
- Li, Q.-L.; Jiang, R.; Ding, Z.-J.; Wang, B.-H. 2019. Spatiotemporal evolution characteristics and phase diagrams of traffic dynamics at a crossroads, *Journal of Statistical Mechanics: Theory and Experiment* 2019: 113403. <https://doi.org/10.1088/1742-5468/ab417b>
- Lighthill, M. J.; Whitham, G. B. 1955. On kinematic waves II. A theory of traffic flow on long crowded roads, *Proceedings of the Royal Society A: Mathematical, Physical and Engineering Sciences* 229(1178): 317–345. <https://doi.org/10.1098/rspa.1955.0089>
- Payne, H. J. 1971. Models of freeway traffic and control, *Mathematical Models of Public Systems* 1: 51–61.
- Richards, P. I. 1956. Shock waves on the highway, *Operations Research* 4(1): 42–51. <https://doi.org/10.1287/opre.4.1.42>
- Shen, W.; Zhang, H. M. 2009. On the morning commute problem in a corridor network with multiple bottlenecks: Its system-optimal traffic flow patterns and the realizing tolling scheme, *Transportation Research Part B: Methodological* 43(3): 267–284. <https://doi.org/10.1016/j.trb.2008.07.004>
- TRB. 2010. *Highway Capacity Manual*. Transportation Research Board (TRB) Washington, DC, US. 1650 p.
- Treiber, M.; Kesting, A. 2012. Validation of traffic flow models with respect to the spatiotemporal evolution of congested traffic patterns, *Transportation Research Part C: Emerging Technologies* 21(1): 31–41. <https://doi.org/10.1016/j.trc.2011.09.002>
- Wang, L.; Chen, H.; Li, Y. 2014. Transition characteristic analysis of traffic evolution process for urban traffic network, *The Scientific World Journal* 2014: 603274. <https://doi.org/10.1155/2014/603274>
- Yang, Y.; Cao, J.; Qin, Y.; Jia, L.; Dong, H.; Zhang, A. 2018. Spatial correlation analysis of urban traffic state under a perspective of community detection, *International Journal of Modern Physics B* 32(12): 1850150. <https://doi.org/10.1142/s0217979218501503>
- Zhang, H. M. 1998. A theory of nonequilibrium traffic flow, *Transportation Research Part B: Methodological* 32(7): 485–498. [https://doi.org/10.1016/s0191-2615\(98\)00014-9](https://doi.org/10.1016/s0191-2615(98)00014-9)
- Zhang, Z.; He, Q.; Tong, H.; Gou, J.; Li, X. 2016. Spatial-temporal traffic flow pattern identification and anomaly detection with dictionary-based compression theory in a large-scale urban network, *Transportation Research Part C: Emerging Technologies* 71: 284–302. <https://doi.org/10.1016/j.trc.2016.08.006>
- Zhu, G.; Song, K.; Zhang, P.; Wang, L. 2016. A traffic flow state transition model for urban road network based on hidden Markov model, *Neurocomputing* 214: 567–574. <https://doi.org/10.1016/j.neucom.2016.06.044>